THE INVESTIGATION OF THE DEPENDENCE OF THE DOUBLE LAYER CAPACITANCE AT THE WATER / NITROBENZENE INTERFACE ON THE SUPPORTING ELECTROLYTES EMPLOYED IN THE AQUEOUS AND ORGANIC PHASE

A Thesis

Presented to the School of Graduate Studies

Addis Ababa University

In Partial Fulfilment of the Requirements for the

Degree of Master of Science in Chemistry

By Tebikie Wondimagegn

June 1994

DEDICATED TO

MY MOTHER AND SISTER

ACKNOWLEDGEMENTS

I would like to express my sincere gratitude to my research advisors Drs. Bernd Hundhammer and Theodros Solomon for identifying the research topic and the keen interest rendered during the period of this research project. I am grateful to them for introducing me to this particular field without which the accomplishment of this material would have been difficult.

I am very much indebted to my friend Ato Mesfin Tesfaye who generously gave of his time and energy in typing, editing and printing out of this material. I wish to express my appreciation to all my friends for their help and encouragement at all stages of this research project.

Financial support from The German Academic Exchange Service (DAAD) is gratefully acknowledged.

Table of contents

List of Figures

List of tables.

1 INTRODUCTION

Studies of electrochemical processes at the interface between two immiscible electrolyte solutions (ITIES) have recently been the subject of a great deal of interest due to the wide range of applications of these systems in chemistry and biology [1]. In particular, these systems have shown to be relevant to ion transfer reaction in ion-selective electrodes, solvent extraction processes and biological membrane phenomena.

The distribution of the ionic and dipolar components across the liquid/liquid interfaces due to an excess of electrical charge on one side of the interface which has to be compensated by the excess opposite charge on the other side of the interface, is usually referred to as the formation of the electrical double layer [2]. Electrical double layers are found in nature, whenever one has systems containing mobile charges, such as electrons, ions or dipoles which distribute themselves under the combined influence of the gradients in chemical and electrical potential [3].

Electrochemical studies at the interface between two immiscible electrolyte solutions date back as far as 1902 [4,5]. The first quantitative treatment of the electrical double layers was done by Verwey and Niessen (as quoted in ref.2). These authors suggested that a layer of solvent molecules (inner layer) separates two ionic space charge regions (diffuse double layer). The Gouy-Chapman theory has been applied to describe this diffuse double layer. This idea was further developed as the modified Verwey-Niessen (MVN) model. This model is explained in detail in the theoretical part. The inner layer can be either free of the ions or the ions are located in the inner layer as specifically adsorbed particles. On the other hand the presence of a diffuse layer at ITIES was neglected by Boguslavsky and Joos and Vanden Bogaert [6 & 7]. They assumed that an ionic monolayer or bilayer is formed at ITIES by specifically adsorbed ions. However, such a situation is likely to occur at higher concentration only.

The concept of an ion free layer at ITIES was investigated by Girault and Schiffrin [8]. They concluded that a continuous change in composition from one phase to the other is a more realistic picture. The thickness of the ion-free layer depends on the polarity of the organic solvent and on the nature of the electrolyte, and for most electrolytes it corresponds to a fraction of the solvent monolayer. Partial solvation effects and interfacial solvent mixing [8] are likely to occur in the inner layer. Samec et al [6] attempted to develop the idea that the probability of finding an ion in the inner-layer region is non zero by considering the MVN model, in which ions were allowed to penetrate the inner layer over some distance. The degree of penetration of ions into the inner layer was found to be a function of ion solvation, e.g., the more hydrated ion the less extensive ion penetration is likely to occur.

The analysis of the space charge regions by the use of the Gouy and Chapman theory underlies the conclusion drawn about the inner layer structure. The GC theory doesn't account for the finite ion size as it was derived by considering the ions as point charges. As a result of this, it would be incorrect to use this theory in predicting the potential drop across the space charge regions at ITIES in the presence of the large ions such as tetraoctylammonium, tetraphenylarsonium or tetraphenylborate.

Most of the experimental results on the electrical double layer at the ITIES were obtained for the ideally polarizable interface, the thermodynamics state of which is controlled by supplying the electrical charge from the outside. This can be achieved by means of a four electrode system [9,10] with two pairs of potential measuring (reference) and current supplying (counter) electrodes. Electrochemical cells can be constructed with a planar [11, 12, 13, 14,15] or spherical [16] liquid/liquid boundary. Flatness of the boundary and geometric configuration of the four electrode system play a role for ensuring the homogeneous polarization of the interface [17 ,18].

The potential difference across the ITIES can be controlled or measured with the help of Luggin capillaries or probes. The potential drop at the ITIES may consist of a more or less significant contribution from the ohmic potential drop across the electrolyte resistance between the tips of the two potential-measuring probes. The ohmic potential drop can be compensated by means of the positive feed back [10] or algebraic subtraction [19, 20] under the potentiostatic or galvanostatic conditions, respectively. This potential drop can be suppressed by increasing the concentration of the base electrolyte. However, the ions of the base electrolyte themselves can be transferred across the interface and contribute to the faradaic current. Thus, the concentration of the base electrolyte should be kept as low as possible in order to minimize the faradic contribution.

The electrical double layer at the ITIES has been investigated by measuring the surface tension [7,8,11,21-26] and the impedance [19,22,27-33] mainly for the water/nitrobenzene [19, 21-25] and the water/1,2 dichloroethane [8,26, 27, 34] systems. The differential capacitance of the electrical double layer at the ITIES should be evaluated through a careful analysis of the experimental impedance data though the surface tension is accessible to a direct measurement.

Impedance investigation is one of the most promising ways of obtaining information about the structure of ITIES. The impedance of the ideally polarizable ITIES was measured by means of the alternating-current bridge [35] or phase-selective detection [17,27, 28, 30, 35, 36]. Samec and Marecek [19,37] tested an alternative impedance method for the evaluation of the ohmic potential drop and capacitance of an ideally polarizable ITIES using the galvanostatic pulse technique.

Buck et al [22] and Gavach et al [24] used the drop-weight and maximum bubble pressure method, respectively to measure the surface tension of the water/nitrobenzene interface in the presence of Bromides of sodium and tetraalkylammonium ions in water and tetraalkylammoniumtetraphenylborate in nitrobenzene. Comparison of the surface charge densities calculated with the help of the GC theory with those experimentally obtained indicated that the potential difference is concentrated in the diffuse double layer.

Electrocapillary curves for the ideally polarizable interface were measured by Kakiuchi and Senda [11,12] in the presence of LiCl in water and TBuATPB in nitrobenzene at different concentration of the electrolytes employed in both phases by the drop-weight/drop-time method using a dropping electrolyte method [11]. The zero charge potential difference was found to be independent of the concentration of both electrolytes. An independent measurement of the potential of the zero charge by the streaming-jet electrode technique [34] gave a value identical with the potential of the electrocapillary maximum. In the absence of specific adsorption, the zero charge potential difference is independent of the type and concentration of both electrolyte for the water/ nitrobenzene and water/1,2-dichloroethane systems. On the contrary, Paleska et al [38] have recently compared the electrocapillary maximum values with those of the streaming maximum potential and the capacitance minimum potential for the TBuATPB(NB) / LiCl(w), TBuATPB (NB+Benzene) / LiCl(w), and TBuATPB(DCE) /LiCl (w) interfaces. The difference among these potential values were remarked upon and discussed for further studies on the polarizability and structure model of the ITIES. The interface between two immiscible electrolyte solutions is not as intensely polarizable as the metal/electrolyte system [39]. As a result, it is possible to observe different potentials of zero charge values depending on the compositions, experimental methods and conditions of the experiment.

The electrocapillary curve for a solution of KCl in water and TBuATPB in 1,2-dichloroethane has been reported by Girault and Schiffrin [40] using a pendant-drop video-image digitizing technique [13]. Results were found to be in good agreement with integrated capacitance data obtained from galvanostatic pulse measurements.

Samec et al [40] applied the weak coupling equations [2] to the primitive model[2] of an ITIES and compared the effect of image forces for the water/nitrobenzene and water/1,2-dichloroethane interfaces. They suggested that the image forces together with the within layer ion correlations are more likely to be responsible for a virtual rise of the experimental capacitance of the water/1,2-dichloroethane over the GC values than the interfacial ion-pairing [40].

The adsorption of 1,2-dilauroyl(DLPC), 1,2-dimyristoyl(DMPC) and 1,2-dipalmitoyl-sn-glycero-3-phosphatidyl choline(DPPC) has been investigated by Senda et al [2] and Samec et al [42, 43] using the impedance technique at the water/nitrobenzene interface. A strong potential dependent adsorption was observed by a decrease in the double layer capacitance at potentials negative to the potential of zero charge.

Senda et al [44] have also studied the adsorption of hexadecyltrymethylammonium and cetyltrymethylammonium ions at the ideally polarizable water/nitrobenzene interface by means of the surface tension and impedance measurements. The adsorption of these cationic surfactants was also found to be dependent on the interfacial potential difference.

Recently, Seno et al [45] investigated the adsorption of poly(oxyethylene)dodecyl ethers (non-ionicsurfactants) at the water/nitrobenzene interface by means of ac impedance measurements. The inner layer capacitance decreased when the surfactants were added to the nitrobenzene phase. The difference in polarity between the water and

the adsorbate could be a resonable physical explanation of the decrease of the inner layer capacitance. The experimental results indicated that all the non-ionic surfactants studied are strongly adsorbed at the water/nitrobenzene interface.

Capacitance data were reported for ideally polarizable interface between the aqueous solution of LiCl and the nitrobenzene soultion of TPenATPB [46], TPhATPB [2, 6, 28], TBuATPB [2, 6, 33, 36], between the aqueous solution of NaBr and the nitrobenzene soultion of TPhAsDcc [6], TBuATPB [2, 6, 29], TPhAsTPB [6], between the nitrobenzene soultion of TBuATPB and the aqueous solution of NaCl [2], KCl [2], RbCl [2], $MgSO_4$ [6] or $MgCl_2$ [28], and between the 1,2-dichloroethane solution of TBuATPB and the aqueous solution of LiCl [27,35,41]. NaCl(w) and TPhAsTPB(NB) were also used to study the double layer capacitance at the water/nitrobenzene interface [30].

Chechirlian et al [47] have shown that the conductivity of the media, the design of the reference electrodes and the geometry of the cell all have a role in affecting impedance measurements at the high frequency limit.

In accordance with the literature, a systematic study of the double layer capacitance hasn't been reported so far. It is the aim of this investigation to study systematically the influence of the supporting electrolytes employed in the aqueous and organic phases on the double layer capacitance(DLC). Nitrobenzene is used as the organic solvent, because it fulfills the requirements for the choice of the non-aqueous solvent. According to Koryta and Vanysek [48], these requirements are listed as follows.

i. The organic solvent must dissolve a small amount of water and Viceversa.
ii. The organic solvent must be sufficiently polar to promote sufficient dissociation of the base electrolyte.

iii. The organic solvent density should differ significantly from the aqueous phase so that a physically stable liquid/liquid boundary could be formed.

Acetophenone [49], benzonitrile [50,51], chloroform [50,52], nitroethane [53], nitrophenylether [54] and dichloromethane [55] have also been used for the non-aqueous phase to investigate ion transfer across the water/organic solvent interface.

The supporting electrolytes choosen in the non aqueous phase are TOctATPB, THepATPB, THexATPB, TPenATPB and TBuATPB. The aim of this selection is to investigate the influence of the increasing size of the tetraalkylammonium ion on the double layer capacitance.

The supporting electrolytes employed in the aqueous phase are LiF, LiCl, LiBr, and LiI in order to see the influence of the supporting electrolytes anion on the DLC.

2. THEORY

2.1. THE GALVANI POTENTIAL DIFFERENCE ACROSS THE WATER/ORGANIC INTERFACE

The gradients of the chemical potential μ along the generalized coordinate axis is the driving force for processes taking place at the interface between two immiscible electrolyte solutions [56].

$$\text{Driving Force} = -\left(\frac{\partial\mu}{\partial X_i}\right)_{P,T} \quad (1)$$

In the above expression, the coordinate x_i may represent distance, a change in concentration and gravitational field. The chemical potential μ of the particle i can be written as :

$$\mu_i = \mu_i^\circ + RT\ln a_i \quad (2)$$

where μ_i° and a_i are the standard chemical potential and the activity of a particle i under investigation, respectively when long-range coulombic interactions between the particles and all charges which are at a distance to participate in the short-range interactions are considered, one then writes [3]

$$\tilde{\mu}_i = \mu_i + Z_i F\varphi \quad (3)$$

Where $\tilde{\mu}$ is the electrochemical potential of the particle i, φ is the inner potential of the phase.

Combination of equations (2) and (3) yields

$$\hat{\mu}_i = \mu_i^{\circ} + RT\ln a_i + Z_iF\varphi$$

or $$\Delta\hat{\mu}_i = \Delta\mu_i + Z_iF\Delta\varphi \quad (4)$$

The term $\Delta\varphi$ in the above expression is the Galvani potential difference between two phases.

According to Parsons [43, 46], the galvani potential difference at the interface between two immiscible electrolyte solutions can be separated into an ionic and a dipolar contribution. The former results from the space charges distributed between the two diffuse layers present at the charged interface, whereas the latter is the direct consequence of specific orientation of dipolar molecules at the interface, i.e.,

$$\Delta_o^w\varphi = g_o^w(\text{ionic}) + g_o^w(\text{dipolar}) \quad (5)$$

In the absence of specific adsorption at the ITIES, there is no ionic contribution to the Galvani potential difference at the potential of zero charge (PZC). Hence

$$\Delta_o^w\varphi = g_o^w(\text{dipolar}) \quad (6)$$

When the electrochemical potential of the system reaches a minimum, equation (1) approaches zero. Under this circumstance, the electrochemical potential of a species i in the aqueous and organic phases are equal, i.e an equilibrium is established.

$$\hat{\mu}_i(w) = \hat{\mu}_i(o) \quad (7)$$

or

$$\mu_i^o(w) + RT\ln a_i(w) + Z_iF\,\varphi(w) = \mu_i^o(o) + RT\ln a_i(o) + Z_iF\,\varphi(o) \quad (8)$$

Rearrangement of the above equations gives the Galvani potential difference between the two phases.

$$\Delta_o^w\varphi = \left(\frac{\mu_i^o(o) - \mu_i^o(w)}{Z_iF}\right) + \frac{RT}{Z_iF}\ln\frac{a_i(o)}{a_i(w)} \quad (9)$$

$$\Delta_o^w\varphi = \Delta_o^w\varphi_i^\circ + \frac{RT}{Z_iF}\ln\frac{a_i(o)}{a_i(w)} \quad (10)$$

Where $\Delta_o^w\varphi_i^\circ$ is the standard potential difference which is the equilibrium value of $\Delta_o^w\varphi$ at the unit ratio of ion activities. It is closely related to the standard Gibbs energy of ion transfer from the aqueous phase to the organic phase, $\Delta\vec{G}^\circ_{tr,i}$

$$\Delta\vec{G}^\circ_{tr,i} = \Delta_o^w\varphi_i^\circ \times Z_iF \quad (11)$$

2.2 POLARIZABLE AND NON-POLARIZABLE INTERFACES.

Consider the simplest system which is represented by a non-polarizable interface in the presence of a single binary electrolyte partitioned between two immiscible solvents (w) and (o). The equilibrium partition of a single binary electrolyte can be represented as[2]

$$(w),R^+X^-/R^+X^-,(o) \tag{12}$$

Where the stroke represents the interface. At equilibrium

$$\hat{\mu}_{R^+}(w) = \hat{\mu}_{R^+}(o) \tag{13}$$

and $$\hat{\mu}_{X^-}(w) = \hat{\mu}_{X^-}(o) \tag{14}$$

and consequently,

$$\Delta_o^w\varphi = \Delta_o^w\varphi^o_{R^+} + \frac{RT}{F}\ln\frac{a_{R^+}(o)}{a_{R^+}(w)} \tag{15}$$

$$\Delta_o^w\varphi = \Delta_o^w\varphi^o_{X^-} + \frac{RT}{F}\ln\frac{a_{X^-}(w)}{a_{X^-}(o)} \tag{16}$$

addition of equations (15) and (16) gives

$$\Delta_o^w\varphi = \left[\frac{\Delta_o^w\varphi^o_{R^+} + \Delta_o^w\varphi^o_{X^-}}{2}\right] + \frac{RT}{2F}\ln\frac{a_{R^+}(o)a_{X^-}(w)}{a_{R^+}(w)a_{X^-}(o)} \tag{17}$$

The electroneutrality condition requires that

$$CR^{+(o,w)} = CX^{-(o,w)} \tag{18}$$

Hence, equation (17) takes the form

$$\Delta_o^w\varphi = \left(\frac{\Delta_o^w\varphi^o_{R^+} + \Delta_o^w\varphi^o_{X^-}}{2}\right) + \frac{RT}{2F}\ln\frac{\gamma R^+(o)\gamma X^-(w)}{\gamma R^+(w)\gamma X^-(o)} \tag{19}$$

Where γR^+ and γX^- are the activity coefficients of the cation and anion, respectively in their respective phases.

Koryta et al [59] have shown that the system with two different electrolytes ***RX*** and ***SY*** in the phases ***w*** and ***O***, respectively, can have the property of an ideally polarizable electrode(blocking electrode). If both ions of ***RX*** are strongly hydrophilic whereas the ions of ***SY*** are strongly hydrophobic, the standard potential of transfer of the cation(R^+) of the aqueous phase and the anion(Y^-) of the non-aqueous phase are very positive and the potential of transfer of the anion(X^-) of the aqueous phase and the cation(S^+) of the organic phase are negative. Under these conditions there will be a definite potential range, often termed as the potential window at which no ions can be transferred across the interface, thus the interface has the properties of an ideally polarized electrode[60]. The potential difference $\Delta_o^w\varphi$ at the ideally polarizable ITIES has the magnitude controlled by the excess electrical charge in the interfacial region rather than by the activities of the ions. The ideally polarizable interface is useful to study the electrical double layer at the ITIES and to investigate ions whose potential of transfer lies within the potential window.

The ideally polarizable interface between two immiscible electrolyte solutions is analogous to that of an ideally polarized interface between metallic electrode-electrolyte solutions when both interfaces are charged from an external source. In both cases the phases are charged by a supply of charge to or a removal from the interface. In the case of a metallic electrode-electrolyte interface, the charge supplied to or removed from

the metallic side are electrons whereas in the case of an interface of two immiscible electrolyte solutions only ions transport to and from the interface takes place.

2.3 CAPACITANCE AT THE WATER/ORGANIC SOLVENT INTERFACE

The measurements of the dependence of charge and capacity of the interface between two immiscible electrolyte solutions upon its potential is a useful tool for elucidating the structure of the electrical double layer.

For the MVN model [2] the Galvani potential difference $\Delta_{\bullet}^{w}\varphi$ splits into three contributions:

$$\Delta_{o}^{w}\varphi = \Delta_{o}^{w}\varphi_{i} + \varphi_{2^{(o)}} - \varphi_{2^{(w)}} \qquad (20)$$

Where $\Delta_{o}^{w}\varphi_{i}$ is the potential differences across the inner layer and $\varphi_{2^{(o)}}$ and $\varphi_{2^{(w)}}$ are the potential difference across the space charge regions in the phases (o) and (w), respectively. (fig. 1)

In the absence of specific adsorption in the inner layer, the double layer capacitance can be represented as a series combination of the inner layer capacitance C_i and the diffuse double layer capacities C_{2-o} and C_{2-w} [3].

$$C^{-1} = C_{i}^{-1} + C_{2\text{-}o}^{-1} + C_{2\text{-}w}^{-1} \qquad (21)$$

where $C_i = \frac{dq(w)}{d\Delta^{\circ}_{o}\varphi_i}$ is the capacity of the inner layer and

$C_{2-w} = -\frac{dq(w)}{d\varphi_2(w)}$ or $C_{2-0} = -\frac{dq(o)}{d\varphi_2(o)}$ are the capacities of the diffuse layers in the phase (w) or (o), respectively.

For a symmetrical electrolyte the surface charge densities are expressed as [33]:

$$q(o) = -2A^{o}\mathrm{Sinh}\left(\frac{ZF\varphi_2(o)}{2RT}\right) \tag{22}$$

$$q(w) = -2A^{w}\mathrm{Sinh}\left(\frac{ZF\varphi_2(w)}{2RT}\right) \tag{23}$$

and consequently, the capacitances of the diffuse layers take the form:

$$C_{2-0} = \left(\frac{ZFA^{0}}{RT}\right)\mathrm{Cosh}\left(\frac{ZF\varphi_2(o)}{2RT}\right) \tag{24}$$

$$C_{2-w} = \left(\frac{ZFA^{w}}{RT}\right)\mathrm{Cosh}\left(\frac{ZF\varphi_2(w)}{2RT}\right) \tag{25}$$

where $A^{\alpha(w)} = \sqrt{\left(2RT\varepsilon^{\alpha(w)}c^{o}\right)}$ and $\varepsilon^{\alpha(w)}$ is the dielectric constant and C^{o} the bulk concentration of the electrolyte.

If the solvent is approximated by a dielectric continuum, the effect of ion penetration on the double layer capacitance can be estimated by solving the linearized Poisson-Boltzmann equations in all the three regions of the MVN model using boundary conditions[6]. Then the inverse capacitance can be written as[6].

$$C^{-1} = C_i^{-1} + C_d^{-1} + \Delta \tag{26}$$

Where C_i and C_d have their usual meaning. In the linearized form they are expressed by:

$$C_d^{-1} = (\varepsilon_0 \varepsilon^w \kappa^w)^{-1} + (\varepsilon_0 \varepsilon^o k^o)^{-1} \quad (27)$$

$$C_i^{-1} = (\varepsilon_o \varepsilon^i)^{-1} \delta \quad (28)$$

Where k^{-1} is the Debye screening length

$$k^{-1} = \left(\frac{F^2}{\varepsilon_o \varepsilon RT} \sum_i Z_i^2 C_i \right)^{-1/2} \quad (29)$$

The subscript i refers to the inner layer and δ represents the thickness of the inner layer. The parameter Δ, which accounts for the ion penetration, is given by:

$$\Delta = \left(\varepsilon^i \varepsilon_0 \kappa^i \right)^{-1} \left[\frac{\left(1 - s^2\right) \tanh\left(\kappa^i \delta\right)}{1 + s \tanh\left(\kappa^i \delta\right)} - \kappa^i \delta \right] \quad (30)$$

where $S = \left(\varepsilon^i \kappa^i / \varepsilon^o \kappa^o \right)$

In the absence of ion penetration, the Debye screening length approaches infinity, i.e. (k^i = 0, S=0, Δ=0) and consequently, $C^{-1} = C_i^{-1} + C_d^{-1}$. For $k^i \neq 0$ the parameter Δ is negative and the inverse capacitance is reduced which corresponds to a drop in the inner layer potential difference.

2.4 REPRESENTATION OF THE WATER/ORGANIC SOLVENT INTERFACE

The water/organic solvent interface can be represented by the equivalent circuit shown in fig.2, where R_S is the solution resistance between the tips of the Luggin capillaries, C the capacity of the interface and Z_F the faradaic impedance for the transfer reactions of the electrolyte ions. Since ion transfer is a rather fast process, the faradaic impedance can be approximated by the corresponding Warburg impedance.

The impedance of the ITIES can be evaluated from the in-phase and quadrature components of the sinusoidal current flowing through the interface[19].

$$Z = V_m\left[I^2(0^\circ) + I^2(90^\circ)\right]^{-\frac{1}{2}} \tag{31}$$

where V_m is the amplitude of the applied sinusoidal voltage. The phase shift between the applied and measured signal is given by:

$$\theta = \tan^{-1}\left[\frac{I(90^\circ)}{I(0^\circ)}\right] \tag{32}$$

In the absence of specific adsorption, the real Z' and the imaginary Z'' components of the complex impedance become[33,61]

$$Z' = |Z|\cos\theta = \sqrt{2}Z_w\left[\left(\sqrt{2}\frac{Z_w}{Z_c}+1\right)^2+1\right]^{-1} \tag{33}$$

$$Z'' = |Z|\sin\theta = \frac{\sqrt{2}Z_w\left(\sqrt{2}\dfrac{Z_w}{Z_c}+1\right)}{\left[\left(\sqrt{2}\dfrac{Z_w}{Z_c}+1\right)^2+1\right]} \tag{34}$$

Where $Z_C = (\omega c_d)^{-1}$ is the capacitance of the interface.

Two cases of interest are defined by the conditions: $\omega \rightarrow 0$ and $\omega \rightarrow \infty$. In the first case

$$Z' = R_s + \sqrt{2}Z_\omega \tag{35}$$

$$Z'' = Z' - R_s \tag{36}$$

Therefore at low frequencies the complex plane yields a straight line with an angle of 45^o. In the second case $\omega \rightarrow \infty$, the real and the imaginary components of the interfacial impedance attain their limiting values,

$$Z' = R_s + Z_c^2 / Z_\omega \tag{37}$$

$$Z'' = Z_c = (\omega c_d)^{-1} \tag{38}$$

In this case, there is a complicated relationship between Z'' and Z' and the impedance plot is not very informative[61]. The double layer capacitance was obtained from the capacitance Zc (eq.38) at a chosen frequency ω and potential E.

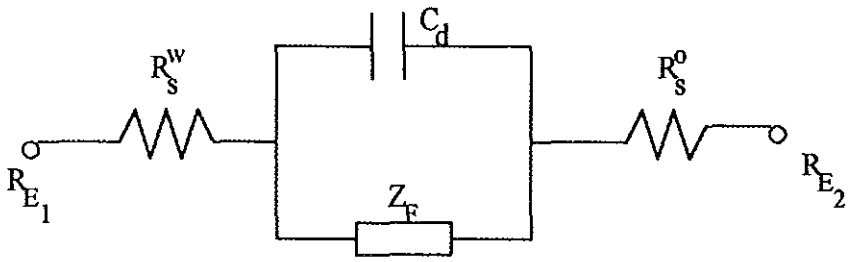

Fig.2 Equivalent circuit for the water/organic solvent interface, C_d is the capacitance interface, Z_F is the faradaic impedance, $R_s^{\circ} + R_s^{w}(R_S)$ is the resistance of the solution between the tips of the Luggin capillaries and R_{E_1} and R_{E_2} are the reference electrodes(Potential measuring Luggin capillaries) in the phase (w) and (o) respectively.

3. EXPERIMENTAL

3.1 CHEMICAL AND PREPARATION OF REAGENTS

The supporting electrolytes for the aqueous phase were LiF, LiCl, LiI (Aldrich, analytical grade) and LiBr (Hopkin and Williams, G.P.R) and were used without further purification. The aquesous solutions were prepared with doubly distilled water immidately before use.

The supporting electrolytes for the organic phase were prepared by mixing 0.01M solutions of the respective tetraalkylammonium bromide with 0.011M solution of sodium tetraphenylborate(Fluka, analytical grade), both dissolved in methanol. Twice the volume of water was added to the mixture. The white precipitate obtained was filtered off and washed continously with doubly distilled water until the test for bromide was negative. The crude product was recrystallized four times. Further details for the purification of the reagents are given in table 1.

A fresh nitrobenzene solution of the supporting electrolytes was prepared from nitrobenzene and the respective tetraalkylammoniumtetraphenylborate. The nitrobenzene was purified by shaking with 10% H_2SO_4 ,10% NaOH and finally with doubly distilled water until the point of neutralization was obtained.

Table 1 Recrystallized supporting electrolytes.

Tetraalkylammonium Tetraphenylborate	Recrystallized form	Yield in		m_p/°C
		g	%	
ToctATPB	n-propanol	3.6	45.82	130-131
THeptATPB	water/acetone	5.9	80.90	145-147
THexATPB	water/acetone	3.9	57.91	160-162
TPenATPB	water/acetone	1.88	29.87	190-193
TBuATPB	used as obtained			235-237

3.2 CELL ARRANGEMENT

Fig.3 shows the diagram of the electrochemical cell which was used for the studies. For both dc and ac cyclic voltammetric investigations, the cell consisted of four electrodes. Similar to the arrangement used in several laboratories [62-64], the higher density organic phase occupied the bottom of the cell, with the aqueous phase above it. The two solutions were brought into contact and a flat water/nitrobenzene interface with a geometric area of $0.71cm^2$ was formed. A U-shaped glass capillary tube which was filled partly with a saturated solution of KCl in water and in which Ag/AgCl electrode was immersed and partly with nitrobenzene solution of the tetraalkylammonium tetraphenylborate was inserted into the teflon body from the bottom. This capillary was used as reference electrode in the non-aqueous phase.

The Ag/AgCl reference electrodes were placed to each side of the interface as closely as possible in order to minimize the ohmic potential drop in the system. Two platinum electrodes served as counter electrodes. The cell was connected to a four electrode potentiostat with IR compensation by means of positive feedback.

The stability of the reference electrode during the experiment was checked by using the perchlorate(ClO_4^-) as an internal standard(reference ion). After ac cyclic voltammetric measurements were completed, $LiClO_4$ was added to the aqueous phase and the ac voltammograms of its transfer from the water to nitrobenzene were determined. In this way, the experimentally obtained potential scale $\Delta_o^w E$ was transformed to a $\Delta_o^w \varphi$ scale.

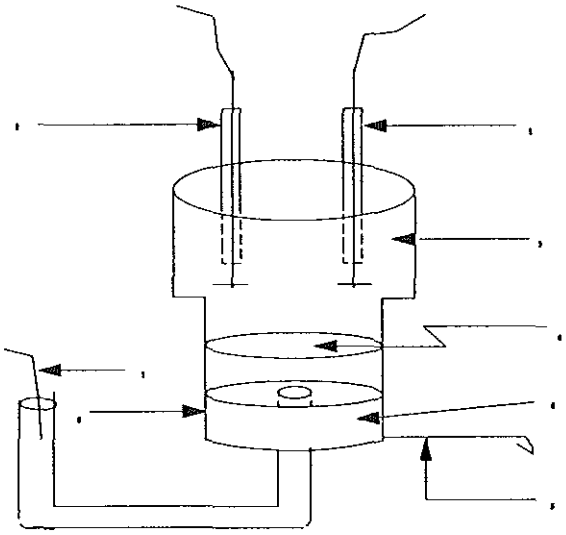

Fig. 3 The cell used in the study

1. Counter electrode(Aqueous phase)
2. Reference electrode(Aqueous phase)
3. Aqueous phase
4. Interface
5. Counter electrode (Organic phase)
6. Organic phase
7. Reference electrode(Organic phase))
8. Teflon body

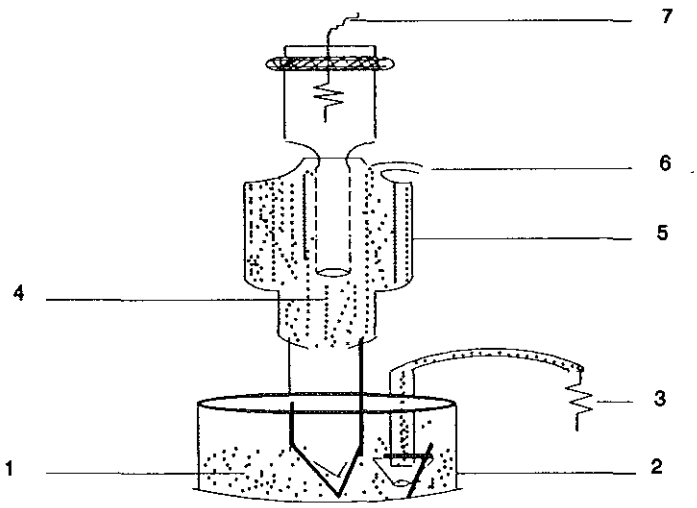

Fig. 4 Diagram of the cell employed for the measurement of the points of zero charge.

1. Organic phase
2. Streaming electrode reserviour
3. Reference electrode for the organic phase
4. Aqueous solution
5. Aqueous solution reserviour
6. Pressure inlet
7. Reference electrode for queous phase

The potential of zero charge was measured by a streaming-jet electrode technique. The diagram of the cell used for the measurement of the potential of zero charge is shown in fig. 4. Its working principle is based on the idea that when the aqueous solutions is allowed to stream from an electrode which is not connected to any external source, the excess charge is carried away and the diffuse double layer remains at its potential of zero charge [34].

3.3 THE ELECTRONIC SET-UP

For dc cyclic voltammetric measurements, a triangular voltage ramp of sweep rate 25mv/s was generated using the MP1036 electroanalzer (Mckee Pederson Instruments). In ac cyclic voltammetric experiments a sinusoidal voltage signal of 1.93mV(rms) from the frequency generator (Tektronix FG 501) was superimposed on the triangular voltage ramp(sweep rate 10 mv/s) and feed to the four electrode potentiostat. The output of the potentiostat was connected to the storage oscilloscope (Tektronix Model 5441) to regulate the proper compensation of the IR drop between the reference electrodes. The IR compensation was set to the nearest point before the potentiostat starts oscillating. The current out put of the potentiostat was also connected to a lock-in-analyzer (PAR Model 5204), which was used for the measurement of the in-phase and the quadrature components of the ac-current flowing through the interface. The output of the lock-in-analyzer was in-turn connected to an x-y recorder.

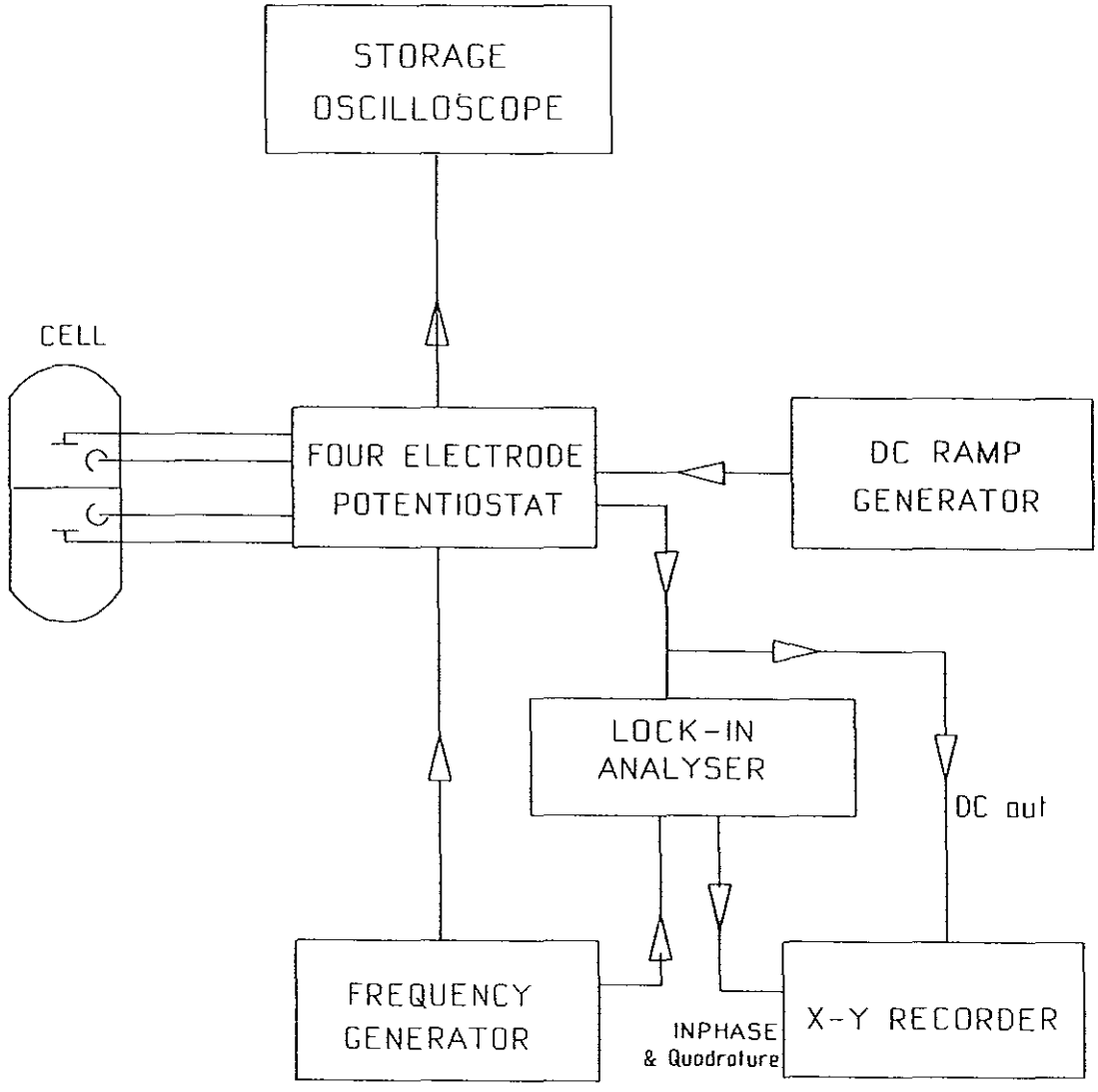

Fig.5 shows the block diagram of the electronic set-up employed for cyclic voltammetry experiments.

4. RESULTS AND DISCUSSION

4.1 VOLTAMMETRIC STUDIES OF THE SUPPORTING ELECTROLYTES EMPLOYED IN THE AQUEOUS AND ORGANIC PHASES.

The principal aim of performing a voltammetric experiment is to determine the applicable potential range within which the boundary (ITIES) behaves as an ideally polarized interface. In the polarizable potential range or " Potential window ", no ions passed the interface and the current is mainly controlled by charging of the interface. However, at the right and left sides of the voltammograms(more negative and positive potentials) the transfer of the base electrolytes prevail. As a consequence, the in-phase and quadrature components of the ac current were measured within the potential window so as to minimize the faradaic contribution.

The influence of the supporting electrolytes anion on the potential window can be seen from fig.6. Based on the standard free energy of the transfer of the individual ions (table 2) presents in the system, it is possible to to suggest that the transfer of TPB^- from nitrobenzene to water cuts off the potential window at positive potentials. However, at negative potentials the transfer of F^-, Cl^-, Br^- and I^- from water to nitrobenzene(curves 1, 2, 3 and 4, respectively) is the limiting charge transfer reaction when LiF, LiCl, LiBr, and LiI are the supporting electrolytes in the aqueous phase, respectively. Therefore at one end of the voltammogram the current is controlled by the transfer of TPB^- from nitrobenzene to water while at the other end of the voltammograms the current is limited by the transfer of the anions of the supporting electrolytes chosen in the aqueous phase.

Fig.6 (curve 1) shows the ac and dc voltammograms obtained at the water / nitrobenzene interface with LiF as supporting electrolyte in water and ToctATPB in nitrobenzene. In the potential range -0.315V - 0.13V the current corresponds mainly to

double layer charging whereas the increasing positive current at potential more positive than 0.13V corresponds to the transfer of TPB^- from nitrobenzene to water while the increasing negative current at potential more negative than -0.315V is due to the transfer of F^- or $TOct^+$ in the reverse direction.

The effect of the supporting electrolytes cation employed in the organic phase on the potential window is also shown in Fig 7. At more positive potentials the transfer of TPB^- from nitrobenzene to water was observed whereas at more negative potentials the transfer of $ToctA^+$, $THepA^+$, $THexA^+$ $TpenA^+$and $TBuA^+$ from nitrobenzene to water (curves 1, 2, 3, 4 and 5, respectively) is the limiting charge transfer reaction when TOctATPB, THepATPB, THexATPB, TPenATPB and TBuATPB are utilized in the non-aqueous phase, respectively. Thus depending on one's interest the applicable potential range can be systematically shortened/widened by employing a relatively small/large tetraalkylammonium ion in the organic phase.

Fig.8 compares the voltammogram obtained by using TOctATPB as the base electrolyte in nitrobenzene and LiCl in water with the voltammogram where CVTPB has been used. The applicable potential range for the former is extended towards more negative potentials. Hence the introduction of TOctATPB as the base electrolyte for the organic phase may allow the investigation of the transfer of te anions which can't be studied in the presence of CVTPB, TPenATPB, THepATPB, and THexATPB.

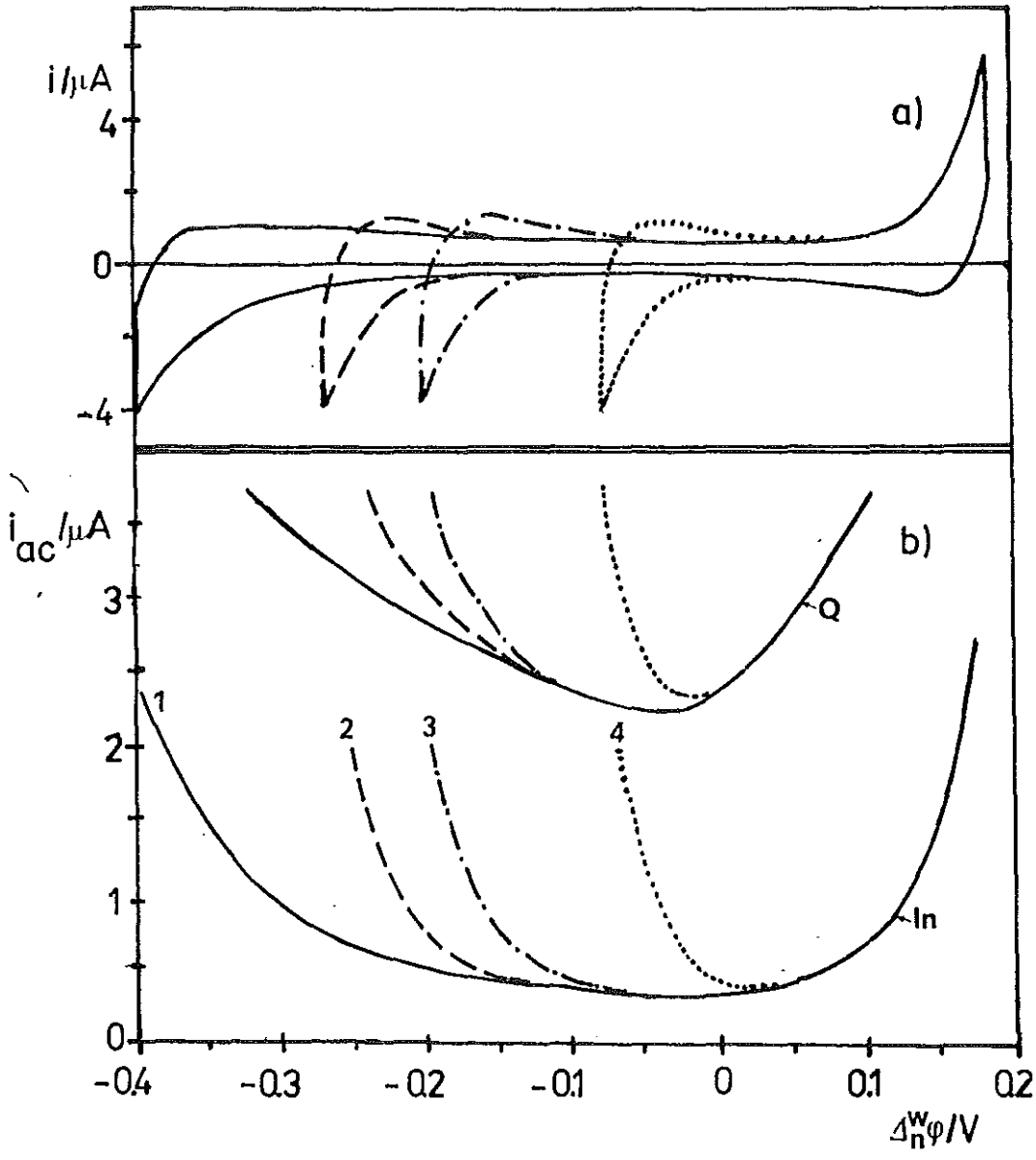

Fig.6. dc (a) and ac (b) cyclic voltammograms for the interface between 0.01M TocATPB in nitrobenzene and 0.01M LiF (1), LiCl (2), LiBr (3) and LiI (4) in water.

Sweep rate: 25 mv/s (a), 10 mv/s (b)

Frequency: 35Hz.

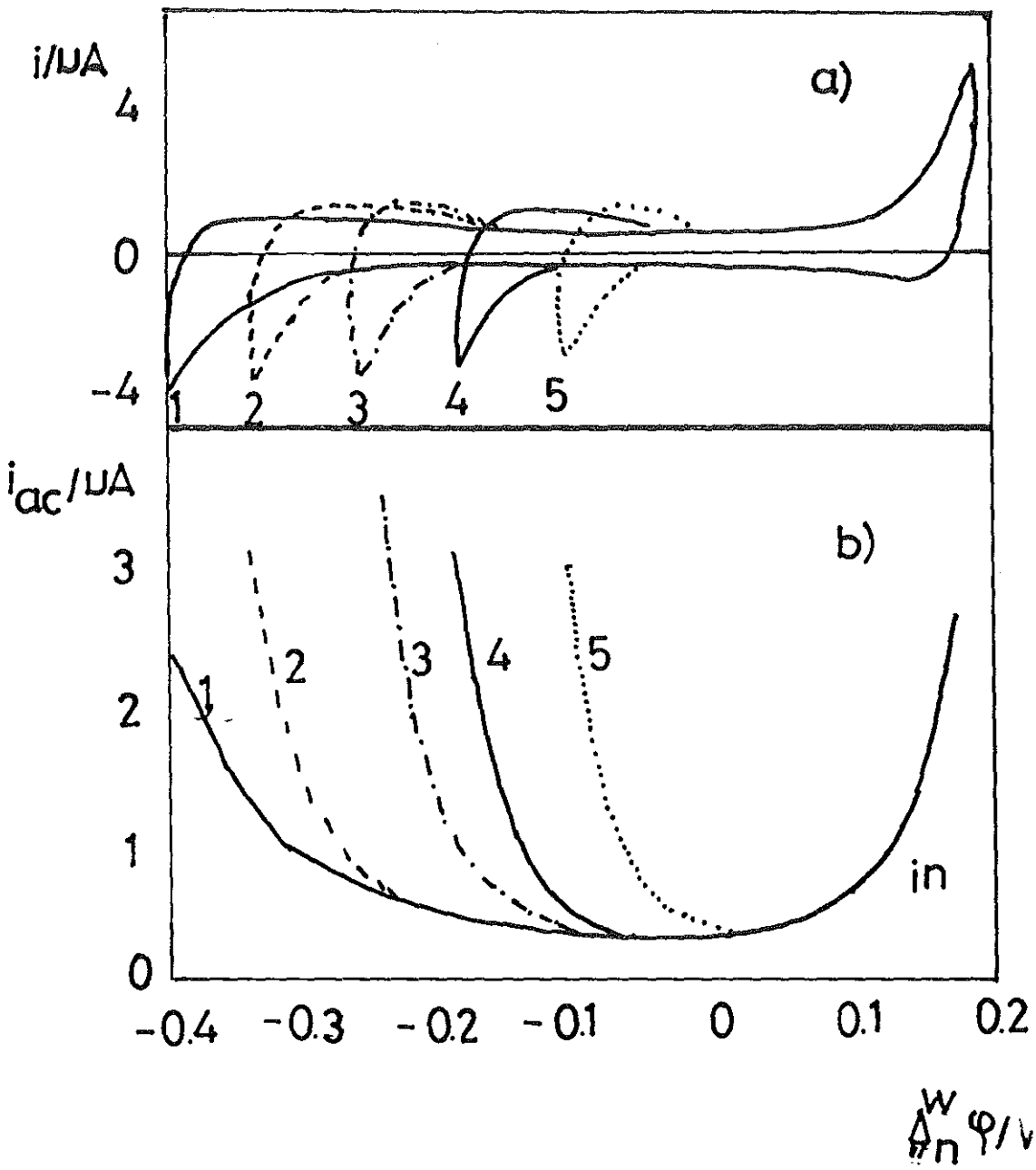

Fig.7. dc (a) and ac (b) cyclic voltammograms for the interface between 0.01M LiF in water and 0.01M TOctATPB (1), THeptATPB (2), THexATPB (3), TPenATPB (4) and TBuATPB (5) in nitrobenzene.

Sweep rate: 25 mv/s (a), 10 mv/s (b)

Frequency: 35Hz.

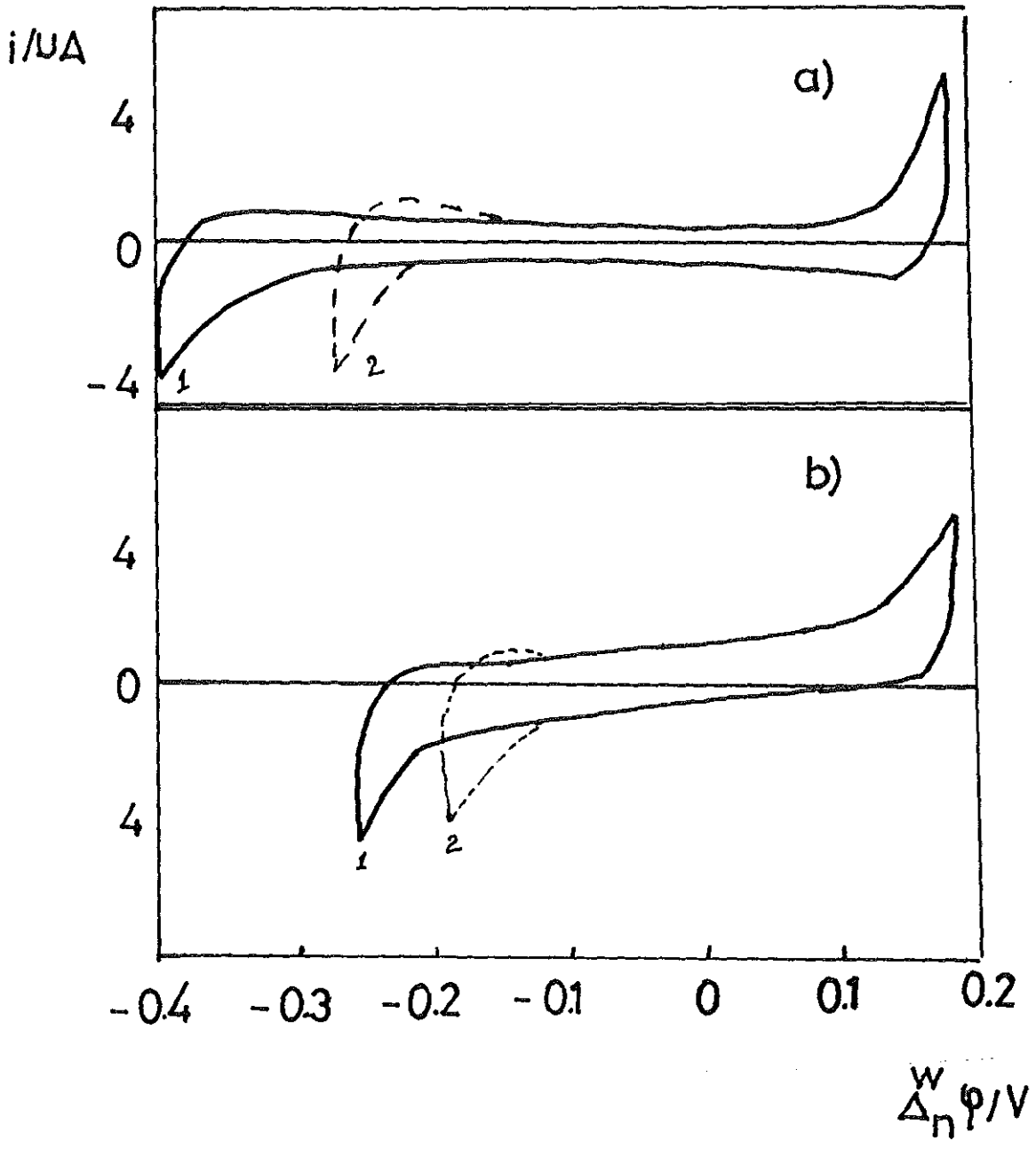

Fig.8. Cyclic Voltammograms of the base electrolytes:0.01M LiCl in water and 0.01M TOctATPB in nitrobenzene (a)[2], and 0.01M CVTPB in nitrobenzene (b)[2]; at sweep rate of 25 mv/s

Table 2 Standard Gibbs energies of transfer from water to nitrobenzene, $\Delta G_{tr}^{o,w\to o}$, and of the standard electrical potential difference between these phases [65]

ION	$\Delta G_{tr}^{o,w\to o}$ / KJ mol^{-1}	$\Delta_o^w\varphi^o$/V
Li^+	38.2	0.3
Na^+	34.2	0.354
K^+	23.4	0.242
Rb^+	19.4	0.201
I^-	18.8	-0.195
Br^-	28.4	-0.295
Cl^-	31.4	-0.324
F^-	44.0	-0.454
TPB^-	-35.9	0.372

To verify the the voltammetric measurements with the extraction data, as an example, the change in the peak potential difference of the I^- and Br^- was measured from the cyclic voltammogram(fig.1), i.e $\Delta_o^w\varphi_{I^-} - \Delta_o^w\varphi_{Br^-} = 0.125V$. The difference between the standard electrical potential of I^- and Br^- is then calculated from table 2 as follow.

$$\Delta_o^w\varphi^oI^- - \Delta_o^w\varphi^oBr^- = 0.100V$$

Therefore ,as shown above, the difference between these two values is small in comparison to the different values of the standard Gibbs energies of transfer reported by different authors.

4.2 THE EVALUATION OF THE DLC FROM EXPERIMENTAL DATA

The investigation of the double layer capacitance was carried out by ac cyclic voltammetry while dc cyclic voltammetry, as discussed earlier, was used to determine the applicable potential range. In ac cyclic voltammetry the in-phase and the quadrature components of the ac current were recorded as a function of potential at different

frequencies. They were transformed into a complex impedance Z using equation(31). The real Z' and the imaginary Z'' components of the complex impedance can be obtained using equations (33) and (34), respectively.

Impedance plot for an aqueous solution of 0.01M LiCl and a nitrobenzene solution of 0.01M TOctATPB is shown in fig.9. The small uncompensated solution resistance can be determined by extrapolation of the impedance plot to $\omega \rightarrow \infty$. The plot indicates the absence of a semicircle or semi-ellipse which is characteristic for a slow faradaic or electrochemical adsorption step, respectively [61]. Therefore this verifies the assumption made in the theoretical part,

i.e $Z_F = Z_W$ and $R_a = 0$ where R_a is the adsorption resistance.

Fig.10 shows an example of the plot of the imaginary impedance versus ω^{-1} at three different potentials for the system consisting of 0.01M LiCl(w) and 0.01M TOctATPB(NB). As expected from theory a linear relationship is obtained. From the slope of the plot, the differential capacitance was evaluated according to equation (38). The differential capacitance of the other supporting electrolytes employed in the aqueous and organic phase has been evaluated in the same way.

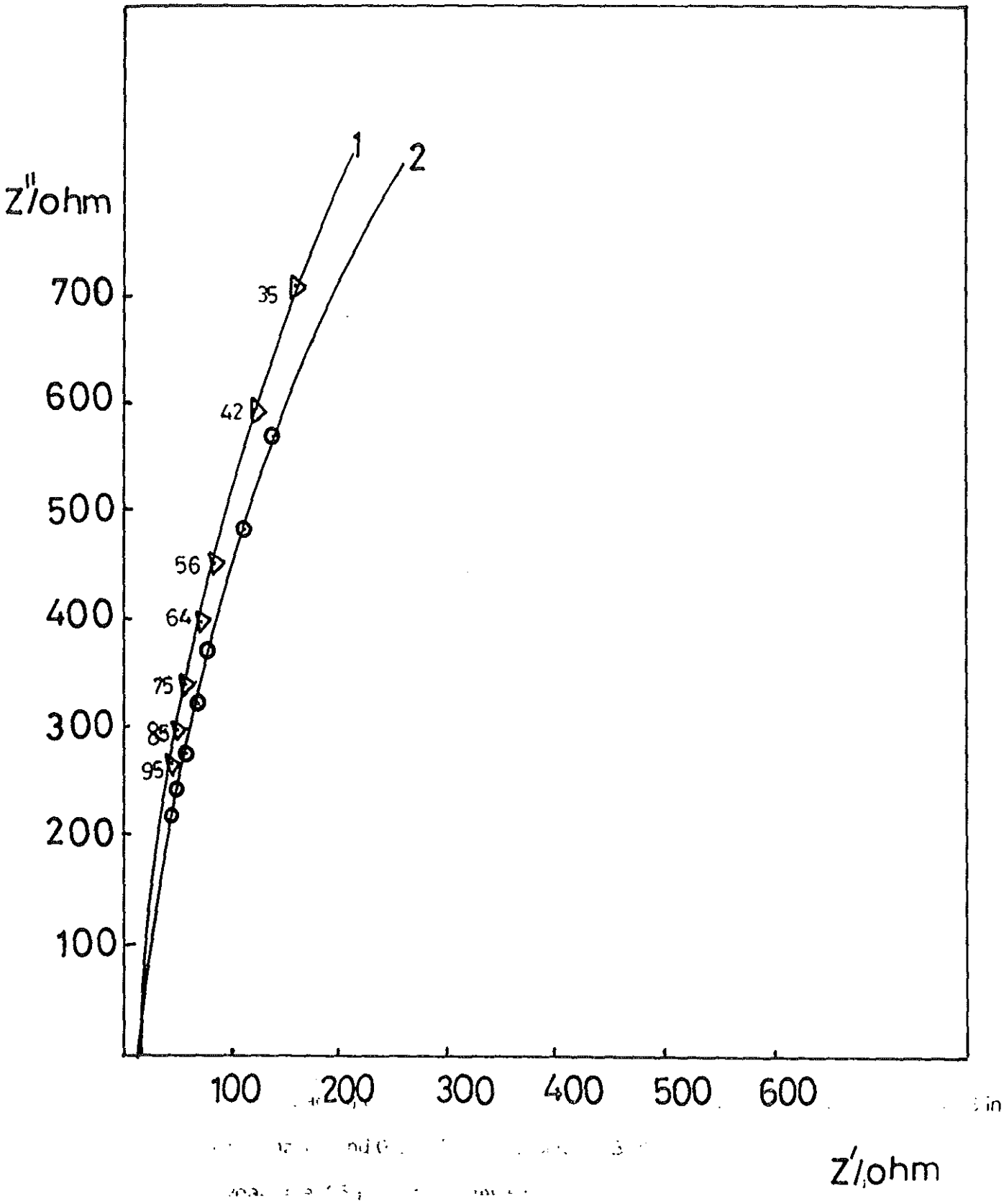

Fig.9. Impedance plot for the interface between 0.01M TOctATPB in nitrobenzene and 0.01M LiCl in water at two different potentials (1):$\Delta\varphi$ = -30 mv, (2): $\Delta\varphi$ = -160 mv. Numbers on the line indicate the frequency in Hertz.

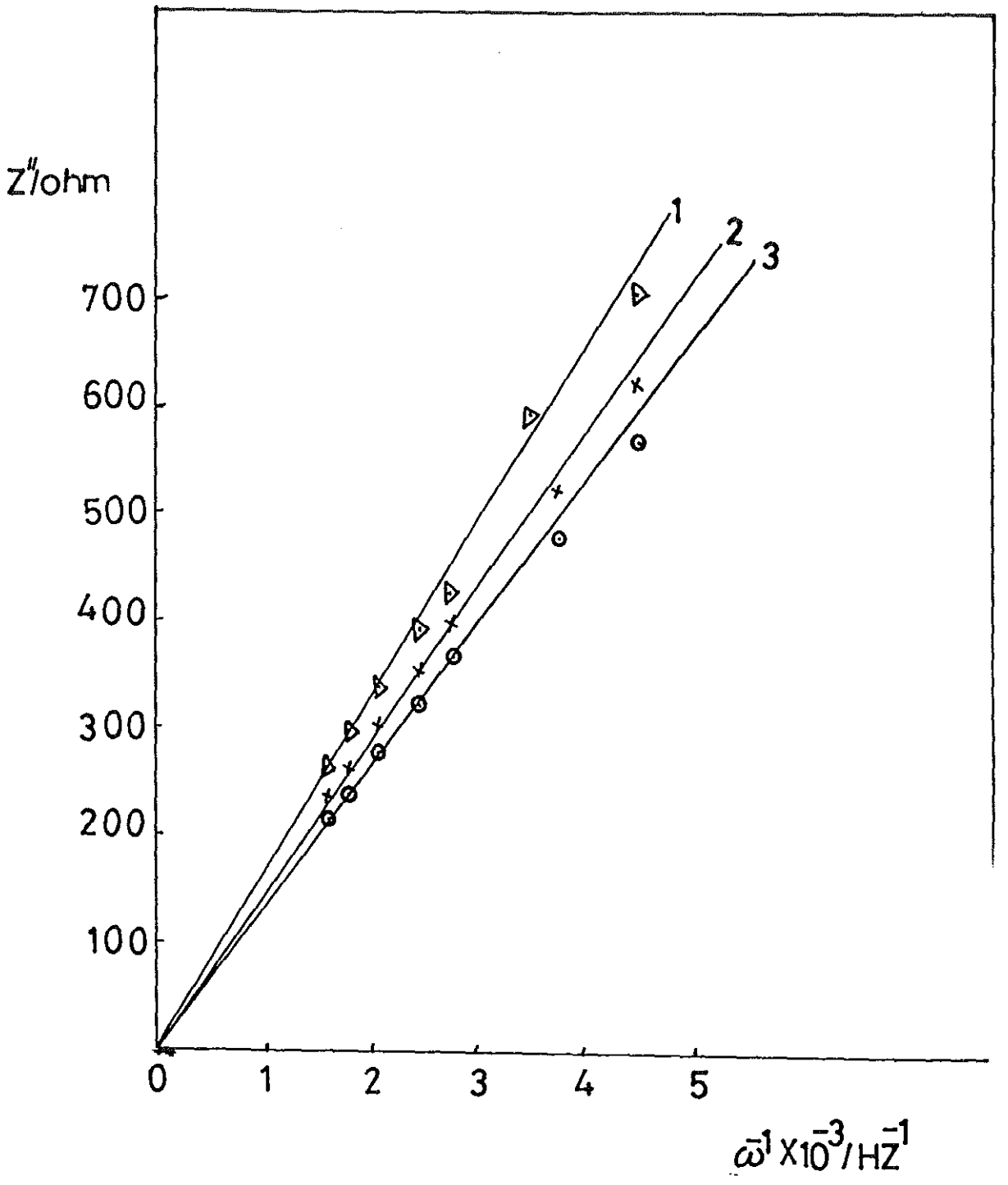

Fig. 10. Plot of Z'' Vs.ω^{-1} for the system: 0.01M LiCl in water and 0.01M TOctATPB in nitrobenzene at different potentials (1): $\Delta\varphi$ = -30 mv , (2): $\Delta\varphi$ = 40 mv , (3): $\Delta\varphi$ = 160 mv.

4.3 CAPACITY MINIMUM AND POTENTIAL OF ZERO CHARGE

The potential corresponding to the minimum capacitance has been determined from the plot of the differential capacitance against the appied potential whereas the streaming potential, as mentioned in the experimental section, was measured by a streaming-jet electrode. In the absence of specific adsorption, the potential of the capacity minimum corresponds to the potential of zero charge.

The Galvani potential of the streaming and of the capacity minimum are listed in table 3 for a system comprising a nitrobenzene solution of TOctATPB and an aqueous solution various supporting electrolytes. The base electrolytes have comparable streaming potential, potential of minimum capacity and capacity minimum. The difference between them are within the range of the experimental error. However, the deviations are not systematic as shown in table 3 for various supporting electrolytes in the aqueous phase. The difference between the streaming potential and potential of the differential capacity minimum for LiBr is in agreement with the values obtained by Paleska et al [53].

Table 4 also illustrates the potential of the streaming electrode and the potential of the differential capacity minimum for the interface between 0.01M LiF(w) and 0.01M various supporting electrolytes in the non-aqueous phase. Similarly the supporting electrolytes in the organic phase have comparable streaming potential and capacity minimum. TOctATPB and TPenATPB have identical streaming potential and potential of differential capacity minimum. The difference between these potentials for TBuATPB is in agreement with the values reported by Paleska et al [38] for systems containing TBuATPB(NB)/LiCl(w), TBuATPB(NB+Benzene)/LiCl(w), and TBuATPB (DCE) / LiCl(w) interfaces.

Therefore, results from this study suggest that the potential of the streaming electrode values, are within reasonable limits, independent of the supporting electrolytes employed in the aqueous and organic phases.

Fig. 11 and 12 shows the plot of the differential capacity versus the applied potential for the supporting electrolytes in the aqueous and organic phases, respectively. As shown in fig 11, the interfacial capacitance increament is larger in the sequence of LiF, LiCl, LiBr, and LiI in the negative branch (in the potential range negative to the capacity minimum) while it remains unchanged in the positive branch. The result indicates that the interfacial capacitance increases in this order due to the interpenetration of ions into the inner layer. The presence of the interpenetration between phases results in the formation of ion pairs which contributes to the surface charge density. The extent of ion pair formation was found to be a function of the standard free energy of transfer of the anions present in the aqueous phase.

Similarly the supporting electrolytes employed in the organic phase influence the differential capacitance in the potential range negative to the capacity minimum. It is apparent from fig. 12 that the drop in the differential capacitance was larger as the size of the tetraalkylammonium ions increases. This may indicate the specific adsorption of ions increases in that order.

Therefore the nature of the supporting electrolytes present in the aqueous and organic phase influences systematically the differential double layer capacitance in the negative branch. However, at potential in the neighborhood of the capacity minimum, the change in the differential capacitance of the supporting electrolytes is small indicating that the interpenetration /specific adsorption of ions at the capacity minimum is negligible.

Fig. 13 shows a comparison of the experimental capacitance with that calculated using the GC theory for systems consisting of LiCl(w) / TBuATPB(NB) and LiCl(w) /

TOctATPB(NB). A drop in the experimental capacitance from the GC theory was observed when the size of tetraalkylammonium ion increases. This effect can be ascribed to the formation of an inner layer at the interface with a finite capacitance. As a consequence, the GC theory overestimates the capacitance of the diffuse layer when tetraalkylammonium ions whith large ionic radii are employed in the non-aqueous phase. The wide discrepancies between theoretical predictions and experimental results are due to the assumption that ions are considered as point charges in deriving the GC theory.

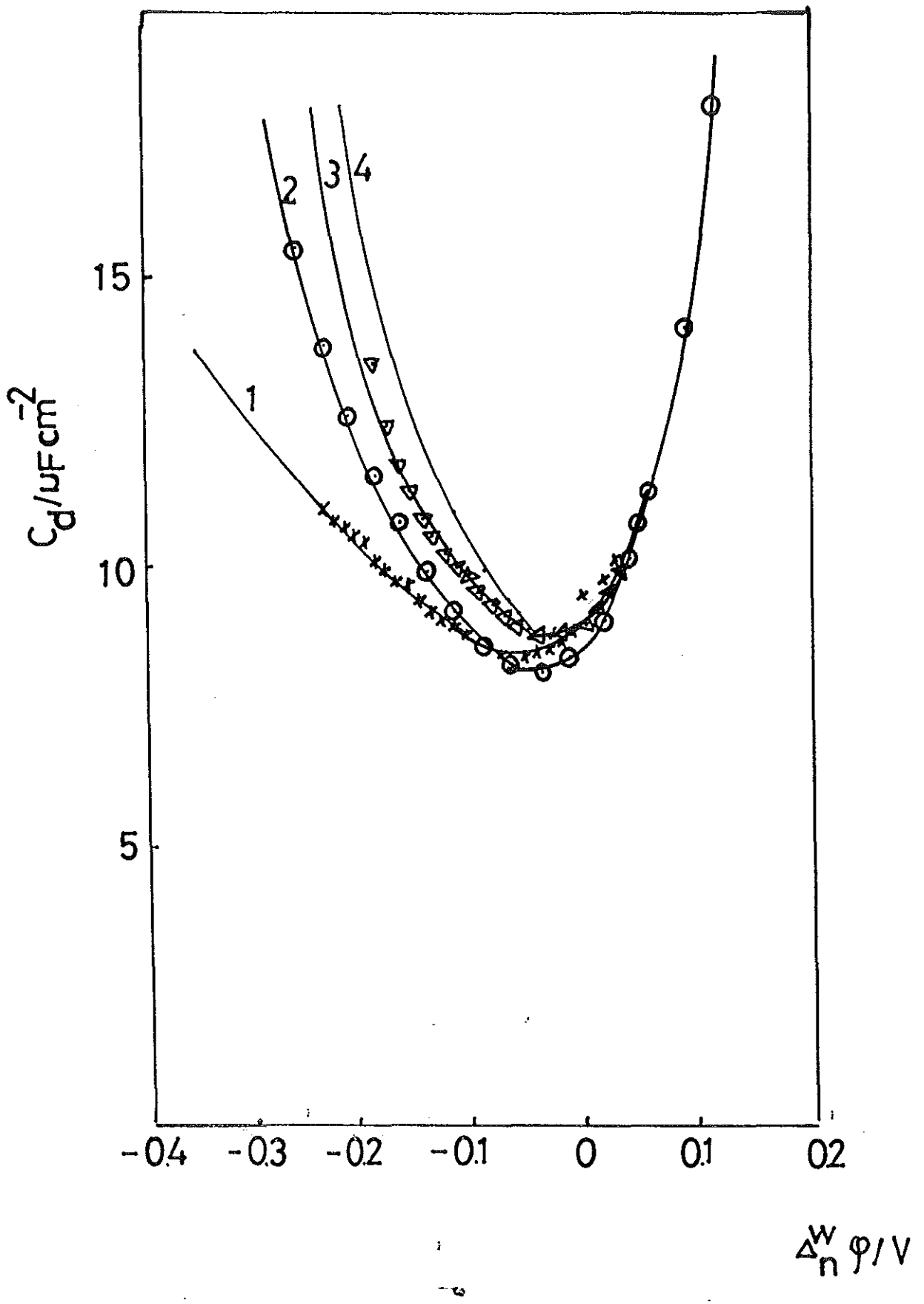

Fig.11. Differential capacitance C of the double layer at the interface between 0.01M
LiCl (2), LiBr (3) and LiI (4) in water and 0.01M TOctATPB in nitrobenzene.

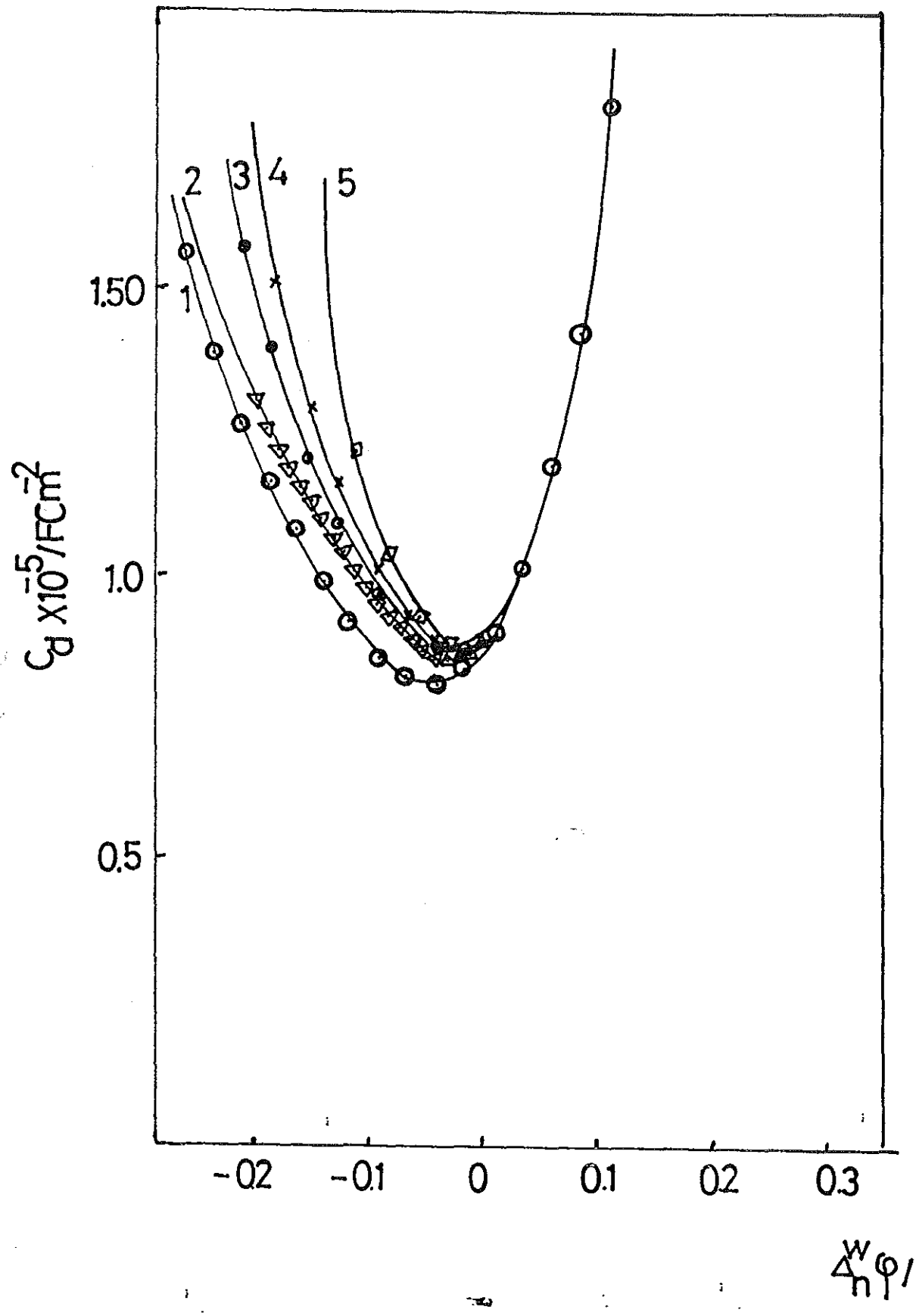

Fig.12. Differential capacitance C of the double layer at the interface between 0.01M LiCl in water and 0.01M TOctATPB (1), THeptATPB (2), THexATPB (3), TPenATPB (4) and TBuATPB (5) in nitrobenzene

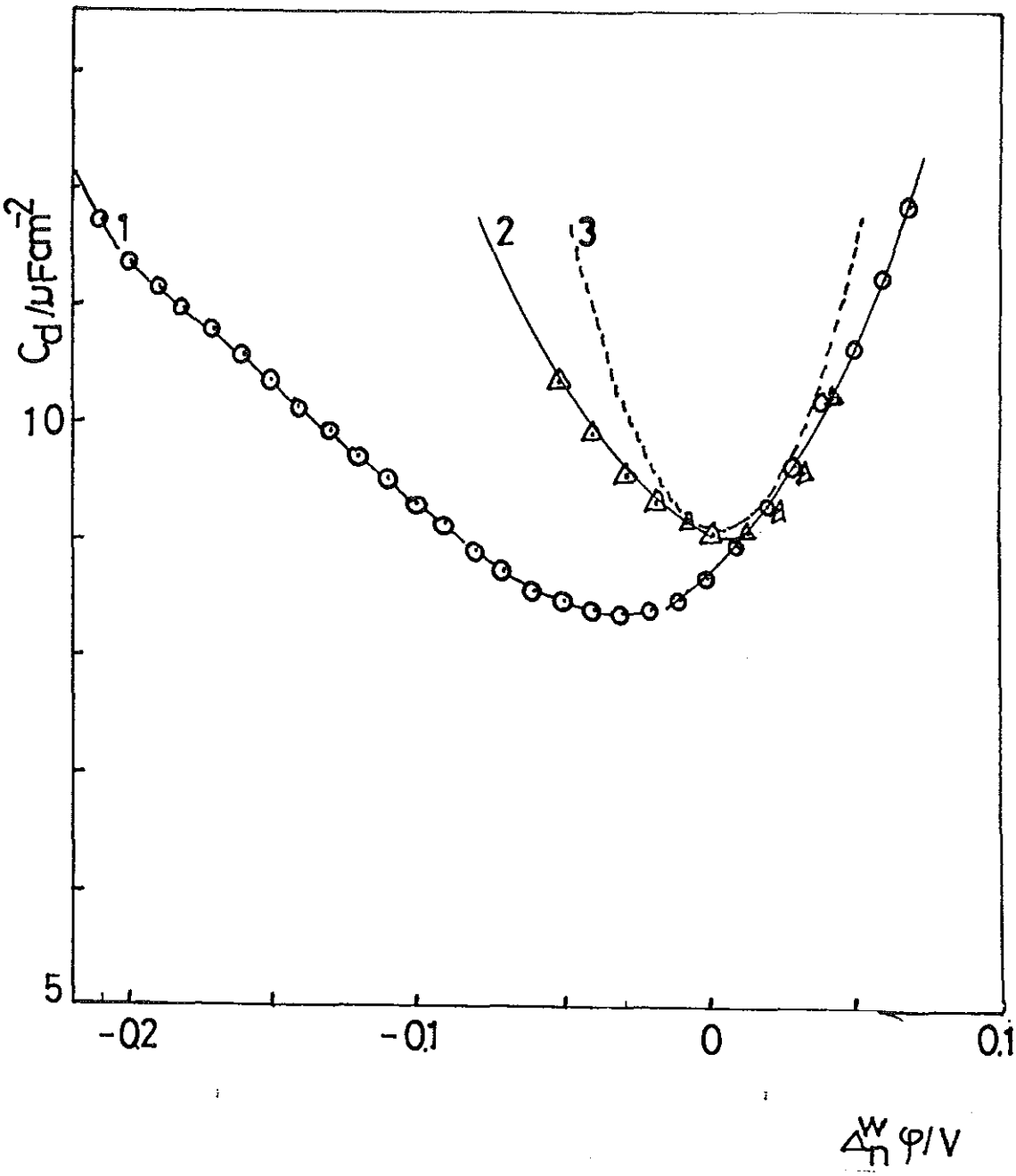

Fig.13. Differential capacitance C of the double layer at the interface between 0.01M LiCl in water and 0.01M TOctATPB (1) and TBuATPB (2). Dashed lines (3) : Capacitance of the diffuse layer calculated with the GC theory assuming that φ_i = constant= 0.

5 CONCLUSION

Ac cyclic voltammetry has been used for the investigation of the double layer capacitance(DLC) at the water/nitrobenzene interface dc cyclic voltammetry has also been used to determine the applicable potential range. The span of the potential window was found to be a function of the standard free energies of transfer of the individual ions present in the system. Attempts have been made to verify the voltammetric experiment with those calculated using the extraction data. The $\Delta\Delta\varphi$ values measured from the cyclic voltammograms and the $\Delta\Delta\varphi^{\circ}$ values calculated from the extraction data are within reasonable limits.

The values of the potential of zero charge measured by the streaming-jet electrode are negative for all the supporting electrolytes employed in the aqueous and organic phases. In both cases, the deviations are not systematic indicating that the streaming potential is independent of the nature of the ions present.

However the measured differential capacitances depend on the nature of the supporting electrolytes used in both phases. Unlike the sreaming potentials the deviations are systematic and not random. Attempts have also been made to correlate the experimental capacitance with those calculated using the GC theory. From the studies made, it was possible to conclude that the GC theory fails to describe the capacitance of the diffuse layer in the presence of a large tetraalkylammonium ion in the non-aqueous phase.

6. REFERENCES

1. M. Senda, T. Kakiuchi, T. Osaki, *Electrochim. Acta,* 36 (1991) 253.
2. Z. Samec, *Chem. Review*, 88 (1988) 617.
3. H. Eyring, *Physical Chemistry an Advanced Treatise*, academic press, New York, vol. IXA , pp 167-246.
4. W. Nernst and E.H. Riesenfeld, *Ann. Phys.*, 8 (1902) 600.(see ref.2).
5. E.H. Riesenfeld, *Ann. Phys*, 8 (1902) 609.(see ref. 2).
6. Z. Samec, V. Marecek and D. Homolka, *J. Electroanal. Chem.*, 187 (1985) 31.
7. P. Joos and R. Vanden Bogaert, *J. Colloid Interface Sci.*, 56 (1976) 206.
8. H.H. Girault and D.J. Schiffrin, *J. Electroanal. Chem.*, 150 (1983) 43.
9. C. Gavach and F. Henry, *J. Electroanal. Chem.*, 54 (1974) 361.
10. Z. Samec, V. Marecek and J. Weber, *J. Electroanal. Chem.*, 100 (1979) 841.
11. T. Kakiuchi and M. Senda, *Bull. Chem. Sos. Jpn.*, 56 (1983) 1322.
12. T. kakiuchi and M. Senda, *Bull. Chem. Soc. Jpn.*, 56 (1983) 1753.
13. H.H. Girault and D.J. Schiffrin and B. D. V. Smith, *J. Electroanal. Chem.*, 137 (1982) 207.
14. J. Koryta, P. Vanysek and M. Brezina, *J. Electroanal. Chem.*, 67 (1976) 263.
15. Z. Yoshida and H. Freiser, *J. Electroanal. Chem.*, 162 (1984) 307.
16. Z. Samec, V. Marecek, D. Homolka and J. Weber, *J. Electroanal. Chem.*, 99 (1979) 385.
17. O.R. Melroy, W.E. Bronner and R.P. Buck, *Bull. Chem. Soc. Jpn.*, 130 (1983) 373.
18. T. Osakai, T. Kakutani and M. Senda, *Bull. Chem. Soc. Jpn.*, 57 (1984) 370.
19. Z. Samec and V. Marecek, *J. Electroanal. Chem.*, 149 (1983) 185.
20. Z. Samec and V. Marecek, *J. Electroanal.Chem.*, 200 (1986) 17.
21. C. Gavach, P. Seta and B.D' Epenoux, *J. Electroanal. Chem.*, 83 (1977) 225.

22. J.D. Reid, O.R. Melroy and R.P. Buck, *J. Electroanal. Chem.*, 147 (1983) 71.

23. T. Kakiuchi and M. Senda, *Bull. Chem. Sos. Jpn.*, 56 (1983) 277.

24. M. Gross, S. Gromb and C. Gavach, *J. Electroanal. Chem.*, 89 (1978) 29.

25. C. Gavach, P. Seta and B. D' Epenoux, *J. Electroanal. Chem.*, 95 (1979) 191.

26. H.H. Girault and D.J.Schiffrin, *J. Electroanal. Chem.*, 179 (1984) 277.

27. P. Hajkova, D. Homolka, V. Marecek and Z. Samec, *J. Electroanal. Chem.*, 151 (1983) 277.

28. P. Hajkova, D. Homolka, V. Marecek and Z. Samec, *J. Electroanal. Chem.*, 159 (1983) 233.

29. D. Homolka, V. Marecek and Z. Samec, *Farad. Disc. Chem. Soc.*, 77 (1984) 197.

30. J.D. Reid, P. Vanysek and R.P. Buck, *J. Electroanal. Chem.*, 161 (1984) 1.

31. J.D. Reid, P. Vanysek and R.P. Buck, *J. Electroanal. Chem.*, 170 (1984) 109.

32. T. Osakai, T. Kakutani and M. Senda, *Bull. Chem. Soc. Jpn.*, 57 (1984) 370.

33. Z. Samec, V. Marecek and D. Homolka, *J. Electroanal. Chem.*, 126 (1981) 121.

34. H.H. Girault and D.J. Schiffrin, *J. Electroanal. Chem.*, 161 (1984) 415.

35. G. Geblewicz, Z. Figaszewski and Z. Koczorowski, *J. Electroanal. Chem.*, 177 (1984) 1.

36. F. Silva and C. Moura, *J. Electroanal. Chem.*, 177 (1984) 317.

37. Z. Samec and V. Marecek, *J. Electroanal.Chem.*, 185 (1985) 263.

38. Z. Koczorowski, I. Paleska and W. Wawrzynezac, *J. Electroanal. Chem.*, 280 (1990) 439.

39. Z. Koczorowski, *J. Electroanal. Chem.*, 190 (1985) 257.

40. H.H. Girault and D.J. Schiffrin, *J. Electroanal. Chem.*, 170 (1984) 127.

41. Z. Samec, V. Marecek, K. Holub, S. Racinsky and P. Hajkova, *J. Electroanal. Chem.*, 225 (1987) 65.

60. P. Vanysek, *Electrochemistry on Liquid\Liquid Interfaces. Lecture Notes in Chemistry*, Springer-Verlag, Berlin, 1985.

61. D.D. Macdonald, *Transient Techniques in Electrochemistry*, Plenum Press, New York and London, 1977.

62. D. Homolka and V. Marecek, *J. Electroanal. Chem.*, 112 (1980) 91.

63. T. Kakutani, T. Osakai and M. Senda, *Bull. Chem. Soc. Jpn.*, 56 (1981) 991.

64. Z. Koczorowski and G. Geblewicz, *J. Electroanal. Chem.*, 139 (1982) 177.

65. Le Q. Hung, *J. Electroanal. Chem.*, 115 (1980) 159